SYNTHESES AND REFLECTANCE ANALYSES OF LUNAR GREEN GLASS COMPOSITIONS: INFORMATION TO IMPROVE UNDERSTANDING OF REMOTELY SENSED SPECTRAL DATA. J. J Gillis-Davis[1], P. G. Lucey[1], J. E. Hammer[2], and B. B. Denevi[3], University of Hawaii at Manoa, Hawaii Institute for Geophysics and Planetology[1], and Geology & Geophysics[2], 1680 East-West Road, POST 503, Honolulu, HI 96744, USA (gillis@higp.hawaii.edu), [3]University of Iowa.

Introduction: Absorption properties of lunar pyroclastic glasses strongly influence spectra of lunar soils and, as a result, spectral remote sensing data of the lunar surface [1,2]. Compositions of many of the >100 lunar pyroclastic deposits identified remotely are poorly constrained [3,4] due to the lack of spectral and space weathering information of lunar pyroclastic glasses. For instance, Hapke modeling [2,5,6] is capable of determining surface composition, grain size, and mineralogy [7,8], however, optical constants do not exist for the range of Fe and Ti contents found in lunar minerals and pyroclastic glasses. Previous spectral studies of lunar synthetic glasses have not reproduced all lunar glass compositions (Fig 1). To this end, synthetic glasses are made with specific compositions (Table 1) and under controlled oxygen fugacity to facilitate study of the relationship between the optical properties of "lunar" glass and FeO, TiO_2 concentrations. Thus, optical constants derived from this work have direct application to radiative transfer modeling of lunar pyroclastic glasses [e.g., 3] and deduction of lunar surface compositions.

Methods: *Sample Synthesis.* The synthetic green and red glass [9] compositions were based on the average lunar glass compositions (Table 1), and were synthesized with reagent-grade carbonate and oxide powders. Flowing H_2-CO_2 gas mixture at 850°C was used to impart an intrinsic fO_2 just above iron-wüstite to simulate lunar conditions. The sample was heated above the liquidus temperature (~1500 °C) quickly (~1 min), and rapidly quenched in a water bath below the furnace. Spectral analysis requires a relatively large quantity (500 mg) of homogenized glass, which obviates the use of the conventional Pt wire loop method. High purity alumina crucibles allow gram-quantities of material to be conditioned and fused at once. The compositional contrast between lunar basalt compositions, which are strongly undersaturated in alumina, and the alumina container materials pose a potential contamination problem. Our preliminary experiments, however, exhibited minimal reaction with the container [9].

Table 1. Compositions of average lunar glasses targeted for synthesis, blue dots in Fig 1.

major oxide	Avg. Green	Avg. Yellow	Avg. Orange	Avg. Red
SiO_2	45.60	41.65	38.24	35.04
TiO_2	0.55	4.85	9.94	14.90
Al_2O_3	7.86	7.63	5.99	5.78
Cr_2O_3	0.51	0.50	0.66	0.89
FeO	19.50	22.42	22.77	22.42
MnO	0.28	0.35	0.31	0.29
MgO	17.11	13.06	13.82	12.81
CaO	8.43	8.41	7.41	7.24
Na_2O	0.19	0.45	0.42	0.36
K_2O	0.01	0.05	0.06	0.14
total	100.04	99.36	99.63	99.86

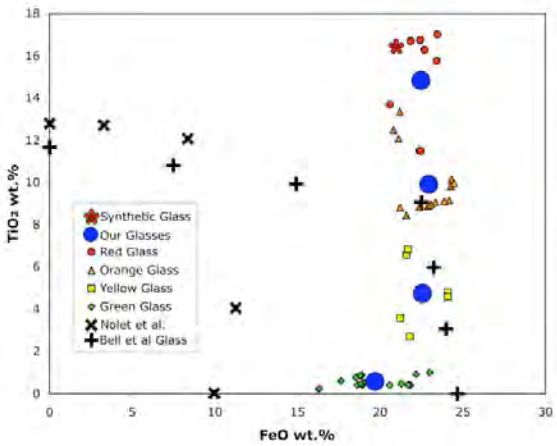

Fig 1. FeO and TiO_2 compositions for our proposed and synthesized glasses, previously made synthetic glasses [9, 11,12], and lunar glass compositions from [13].

Measuring Reflectance and Deriving Optical Constants. Bidirectional reflectance measurements of synthetic lunar glass allow the calculation of optical constants of glasses using Hapke Modelling. The synthetic glass samples have sufficient optical defects at the macroscopic level (Fig 2) to prohibit standard transmission methods for deriving absorption coefficients. Instead, our samples were ground and dry sieved to achieve a fine <53 μm powder. Reflectance measurements were made at the Univ. of Hawaii using an Analytical Spectral Devices© spectrometer, which has a spectral range from 0.35 to 2.5 μm and a spectral resolution of 1 μm. Reflectance measurements are compared against a Spectralon reflectance standards. A quartz-halogen lamp was used as the illumination source, with a 40° incidence angle and 0° emission angle. Additional reflectance measurements will be made at Brown University's Reflectance Laboratory for comparison with our data.

Optical constants were computed from the reflectance values of these powers using the methods of [5,6], as implemented by [7] for deriving mineral optical constants. While other methods are available to derive these constants, these methods require optically high-quality samples. As previously stated, our synthetic samples have macroscopic optical defects that invalidate transmission methods for deriving absorption coefficients.

Results: Our synthetically produced glasses are homogenous with only minor inclusions and nearly crystal/inclusion free (Fig. 2). XRD analyses of powdered synthetic samples determine their composition to be 99% glass. Compositions closely match the composition of the average lunar green and red [9] glasses.

A comparison of reflectance data reveals that the spectral shape of the synthetic green glass more closely matches the spectrum of the Adams [10] green glass than the Pieters green glass (Fig. 3). All the glasses exhibit two bands near 1.0 and 1.9 μm, which corresponds to crystal-field transitions in octahedrally and tetrahedrally coordinated Fe^{2+} ions, respectively [11]. The Fe^{2+} absorption bands of the Adams and synthetic green glass are broad and shallow because of short-range crystal order in glass. In contrast, the asymmetrical 1.0 μm band of the Pieters green glass suggests olivine contamination.

A strong continuum is evident in the 0.4-0.7 μm range. The slope is a charge-transfer band caused by the Fe^{2+}–Ti^{4+} coupled interaction [11]. We observe the shoulder of 400-700 nm slope to be directly related to the Fe^{2+}–Ti^{4+} concentration, which is responsible for the color of the glass. Low-Ti green glasses exhibit a maximum at 600 nm, while high-Ti red glasses have a maximum at 780 nm (Fig. 3).

While the UVVIS slope, band positions, and band shape of the synthetic and lunar [10] glass is similar, a discrepancy exists for reflectance values beyond 600 nm. While natural variation in reflectance values for lunar green glasses are observed (e.g., Pieters and Adams spectral measurements), reflectance values for the synthetic green glass are lower and curiously parallel the red glass reflectance curve (Fig. 3). Hapke modeled reflectance values for glass of similar composition and grain size as the synthetic green glass, and without space weathering exhibit higher reflectance values than measurements of the actual synthetic green glass at longer wavelengths.

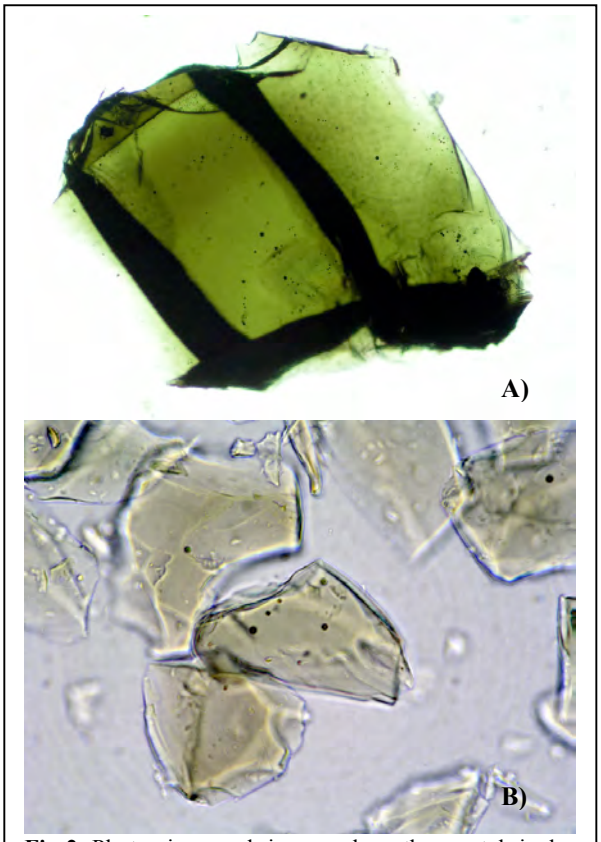

Fig 2. Photomicrograph images show the crystal, inclusion free nature of synthesized green glass at different scales A) the green glass grain is ~0.75 mm. B) green glass grains after sieving, average grain size is 45 μm.

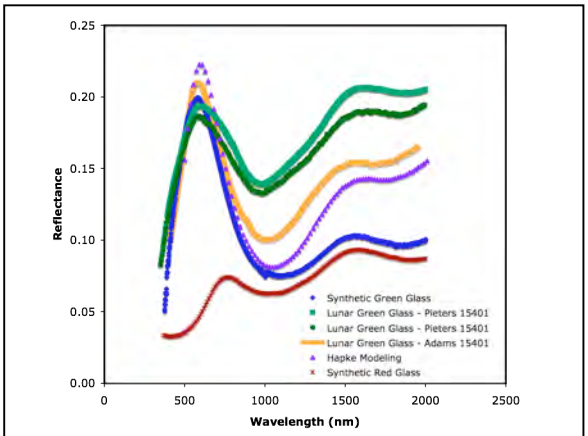

Fig 3. Reflectance of synthetic green glass, Apollo sample 15401, Hapke modeling of similar composition synthetic green glass, and synthetic red glass [9].

Conclusions: We successfully produced green and red glass compositions that are compositionally homogeneous and nearly crystal/inclusion free. Differences in reflectance values between our green glass and lunar green glass could be related to coatings or submicroscopic iron found on and within lunar glasses. The ability to space weather these glasses is needed to test this hypothesis. RELAB data will ascertain the accuracy of our reflectance measurements longward of 800 nm. Spectral differences between the synthetic glass and calculated spectra suggests that either differences in crystal field effects caused by multiple cations contained in the synthetic sample are not being accounted for, or that uncertainties in optical coefficients derived from [11] are significant. Future optical constants derived for the remaining two lunar glass compositions will allow us better resolve these possibilities.

References: [1] Pieters C. M. (1993) Topics in remote sensing 4, pp. 594. [2] Hapke B. (2001) *JGR, 106 (E5),* 10,039-10,073. [3] Wilcox, B. B. et al. (2006) *JGR, 111*, doi:10.1029/2006JE002686. [4] Robinson et al. (2006) *LPSC XXXVII*, #2282. [5] Hapke B. (1993) Theory of reflectance and emittance spectroscopy. Cambridge Univ. Press, Cambridge. [6] Hapke B. (1981) *JGR, 86(B4)*, 3039-3054. [7] Lucey P. G. (1998) JGR, 103, 1703-1714. [8] Lucey (2004) *GRL*, 31 doi:10:1029/2003GL019406. [9] Gillis-Davis, J. J. et al. (2007) *LPSC XXXVIII*, #1443. [10] Adams, J. B. (1974), *JGR*, 4829-4836 [11] Bell P. M. et al (1976) *Proc. Lunar Sci. Conf. 7th*, 2543-2559. [12] Nolet D. A. et al (1979) *Proc. Lunar Sci. Conf. 10th*, 1775-1786. [13] Delano, J. (1986) *Proc. Lunar Sci. Conf. 10th*, D201-D213.